ELSEVIER

Applied Surface Science 127–129 (1998) 111–116

applied surface science

Explosive phase transformation in excimer laser ablation

Kevin H. Song, Xianfan Xu *

School of Mechanical Engineering, Purdue University, West Lafayette, IN 47907, USA

Abstract

This work investigated phase change mechanisms during excimer laser ablation of nickel specimens. Time-resolved measurements were carried out to determine optical properties and the velocity of the laser-ablated plume, the ablation rate per pulse, light scattering from the laser-ablated particles and the size of the laser-ablated particles, in the laser fluence range between 2.5 J cm^{-2} and 10.5 J cm^{-2} (or 100 MW cm^{-2} and 400 MW cm^{-2} for a laser pulse of 26 ns). It was found that normal surface evaporation occurred when the laser fluence was below 5.2 J cm^{-2}. At a laser fluence of about 5.2 J cm^{-2} or higher, the temperature at the target surface approached the critical point. The surface experienced an explosive-type vaporization process, ejecting large size droplets from the molten pool. Further increase of the laser fluence up to 9.0 J cm^{-2} did not significantly change the surface temperature and the velocity and transmission of the laser-ablated plume. Explosive phase transformation was determined to be the main material removal mechanism when the laser fluence was higher than 5.2 J cm^{-2}. © 1998 Elsevier Science B.V.

PACS: 79.20Ds

Keywords: Pulsed laser ablation; Homogeneous nucleation; Explosive phase transformation

1. Introduction

Pulsed laser ablation (PLA) has attracted considerable attention in the last decade. Deposition of thin films of advanced engineering materials such as high temperature superconductors, PZT-based multilayer capacitors and diamond-like carbon films employs the PLA technique for its simplicity and versatility. PLA is also used for micro-scale machining due to the localized heat affected zone (HAZ) caused by short laser pulses. Although PLA has advantages for thin film deposition and micromachining, micrometer size particulates are often generated during the process, causing nonuniform thin film structures or debris. On the other hand, generation of particulates during PLA has been utilized to produce nanometer-size clusters with unique electric, optical or thermal properties. Therefore, understanding the underlying mechanisms of particulate generation in the laser ablation process is critical for PLA related applications.

There are many discussions in the literature on the mechanism of particulate generation during laser ablation. For years, it has been commonly accepted that subsurface superheating is the main cause for particulate formation [1]. According to the subsurface superheating theory, the surface reaches the boiling temperature under laser irradiation and surface vaporization occurs. Due to the loss of the latent heat

* Corresponding author. Tel.: +1-765-494-5639; fax: +1-765-494-0539; e-mail: xxu@ecn.purdue.edu.

PII S0169-4332(97)00619-3

of vaporization at the surface, the temperature at the subsurface region is higher than that at the surface. The pressure beneath the surface is also higher, and thus explosion takes place. Miotello and Kelly [2] and Kelly and Miotello [3] pointed out that the maximum temperature difference between the subsurface region and the surface was negligible when appropriate thermal boundary conditions were used, therefore, the argument of the subsurface superheating was not valid. Alternatively, they introduced the explosive vaporization mechanism for the laser ablation process. According to Miotello and Kelly, when the laser fluence is sufficiently high and the pulse length is sufficiently short, the temperature of the specimen could be raised to well above its boiling temperature. At a temperature of $0.90T_c$ (T_c is the thermodynamic critical temperature), homogeneous bubble nucleation occurs. The surface undergoes a rapid transition from superheated liquid to a mixture of vapor and liquid droplets.

In this work, we carried out experimental studies on phase change mechanisms during pulsed excimer laser ablation of nickel specimens. Time-resolved measurements were performed to determine the velocity and optical properties of the laser-ablated plume in the laser fluence range from 2.5 J cm^{-2} to 10.5 J cm^{-2}. Also, the ablation rate per pulse was estimated by measuring the depth of the ablation crater. These experimental studies showed that, when the laser intensity was over 5.2 J cm^{-2}, transmissivity of the laser beam in the laser-ablated plume and its expansion velocity changed little with laser fluences. Also, when the laser fluence was varied across the 5.2 J cm^{-2} threshold value, there were drastic increases of ablation depth and scattering of laser light from the plume. These experimental results revealed different phase change mechanisms in different laser fluence regimes.

2. Metastable liquid and explosive phase transformation

To illustrate the heating process of a liquid metal by a pulsed laser beam, the phase diagram in the neighborhood of the critical temperature is shown in Fig. 1 [4]. The 'normal heating' line indicates the heating process of a liquid metal when the temperature is below the boiling temperature. At the boiling temperature, the liquid and the vapor phases are in equilibrium, which is shown in Fig. 1 as the binode line calculated from the Clausius–Clapeyron equation. When the surface temperature of a liquid is below or at the boiling temperature, evaporation occurs at the liquid surface, which is a type of heterogeneous evaporation.

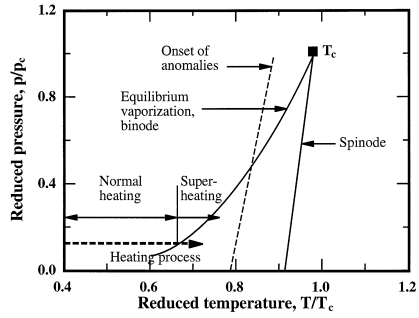

Fig. 1. $P-T$ diagram near the critical point.

Under rapid heating, it is possible to superheat the liquid metal to temperatures above the boiling point [5]. The superheating process is represented by the 'superheating' line in Fig. 1. However, there is a well defined upper limit for superheating of a liquid, the spinode (Fig. 1). The spinode is the boundary of thermodynamic phase stability and is determined by the second derivatives of the Gibbs' thermodynamic potential [6]:

$$\left(\frac{\partial p}{\partial V}\right)_T = 0 \quad \text{and} \quad \left(\frac{\partial T}{\partial S}\right)_p = 0 \tag{1}$$

where V is the specific volume and S is the entropy. Using Eq. (1), the spinode equation can be derived from empirical equations of state such as the van der Waals equation or the Berthelot equation [7]. The derivatives in Eq. (1) are inversely proportional to fluctuations in liquid [8]:

$$\left(\frac{\partial p}{\partial V}\right)_T = -\frac{k_B T}{(\Delta V)^2}$$

and

$$\left(\frac{\partial T}{\partial S}\right)_p = \frac{k_B T^3}{(\Delta H)^2} \tag{2}$$

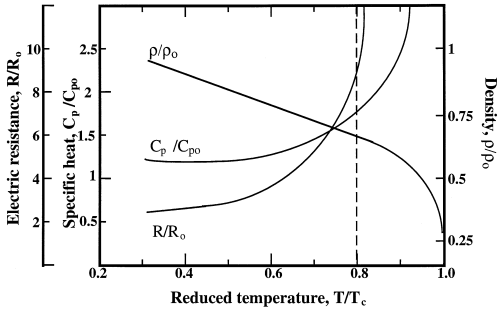

Fig. 2. Typical variations of physical properties of liquid metal near the critical point. The substrate 'o' denotes properties at the normal boiling temperature.

where k_B and H are the Boltzmann constant and enthalpy, respectively. As the temperature approaches the spinode, the fluctuations ΔV and ΔH increase sharply and $(\partial p/\partial V)_T \to 0$, $(\partial T/\partial S)_p \to 0$. A loss of thermodynamic stability occurs. Intense fluctuation begins when the temperature of the metastable liquid approaches $0.8T_c$, which affects physical properties drastically. Fig. 2 shows variations of properties of liquid metal near the critical point [9]. The decrease of density is mainly due to the intensified fluctuation of the specific volume, ΔV, and the increase of the specific heat is mainly due to the increasing fluctuation of enthalpy, ΔH. These drastic property changes are called anomalies, which are also indicated in Fig. 1. Usually, the onset of anomalies concurrently marks the onset of significant reduction or even disappearance of electrical conductivity of a liquid metal [9,10]. Thus, at the onset of anomalies, the liquid metal is transferred from a liquid conductor to a liquid dielectric. Its transmission to optical radiation increases and surface reflectivity decreases [10].

Spontaneous nucleation could occur in a metastable liquid, which affects its stability. According to the Döring and Volmer's theory [11], the frequency of spontaneous nucleation is calculated as:

$$J = NB \exp\left(-\frac{\Delta G_c}{k_B T}\right) \tag{3}$$

where $\Delta G_c = [16\pi\sigma^3]/[3(\rho_0 L_0 \beta)^2]$ is the energy to form critical vapor nuclei at temperature T, B is a function whose dependence on temperature and pressure is much less than exponential, N is the number density of atoms, σ is surface tension, ρ_0 and L_0 are the density of saturated vapor and latent heat of vaporization at the normal boiling temperature T_0, and β is the degree of superheating, defined as $\beta = (T - T_0)/T_0$. According to Eq. (3), the spontaneous nucleation rate increases exponentially with temperature. It has been shown that the frequency of spontaneous nucleation is about 0.1 s^{-1} cm^{-3} at the temperature near 0.89 T_c, but increases to 10^{21} s^{-1} cm^{-3} at $0.91T_c$ [2]. This indicates that a rapidly heated liquid could possess considerable stability with respect to spontaneous nucleation up to $0.89T_c$, with an avalanche-like onset of spontaneous nucleation of the entire high temperature liquid layer at about $0.91T_c$. Therefore, at a temperature of about $0.9T_c$, homogeneous nucleation, or explosive phase transformation occurs.

During pulsed excimer laser heating, radiation energy from the laser beam is transformed to thermal energy within the radiation penetration depth, which is about 10 nm for Ni at the KrF excimer laser wavelength. Superheating is possible since the excimer laser pulse is short, on the order of 10^{-8} s. Within this time duration, the amount of nuclei generated by spontaneous nucleation is small at temperatures below $0.9T_c$, thus the liquid can be heated to the metastable state. Depending on the laser fluence, the target surface can be melted, and the liquid can successively undergo the normal heating process, the superheating process and the explosive phase change. Heterogeneous evaporation always occurs at the liquid surface, however, when the laser intensity is strong enough to induce explosive phase transformation, physical phenomena associated with laser ablation are dominated by explosive vaporization.

3. Experimental study

3.1. Descriptions of the experiments

Experiments are carried out to investigate the excimer laser ablation process. A KrF excimer laser with a wavelength of 248 nm and a pulse width of 26 ns (full width at half maximum, FWHM) is used. The laser fluence is varied from 2.5 J cm^{-2} to 10.5 J cm^{-2}. A 99.94% pure nickel specimen is used as the

ablation target. Experimental procedures and apparatus are described in details in other publications [12,13]. Only a brief description of each experiment is given here.

The optical deflection technique is employed to measure the velocity of the laser-ablated plume. In this experiment, a probing HeNe laser beam traveling parallel to the target surface passes through the laser-ablated plume. The intensity of the probing beam is disturbed due to discontinuity of optical properties across the laser-induced shock wave, and due to scattering and absorption by the plume. The distance between the probing beam and the target surface is incrementally adjusted and the corresponding arrival time of the probing beam fluctuation is recorded. The velocity of the laser-ablated plume can be obtained from the distance–time relation.

Optical properties of the laser-ablated plume are measured. Transmission of the plume at the excimer laser wavelength is measured by a probing beam separated from the excimer laser beam. This probing beam passes through the plume and a small hole (diameter ~ 10 μm) fabricated on the specimen, which is a free-standing nickel foil with a thickness of about 6 μm. The small hole and the thin foil target ensure detection of transmission when the plume thickness is only a few micrometers. Scattering of the laser beam from the plume is measured at different angles. Based on the radiative transfer analysis, the measured angular scattering intensity distribution is used to determine the size of the scattering center in the plume. The total laser energy loss to the ambient due to scattering from the plume and reflection from the target surface is also measured. The laser energy distribution are determined from these measurement results.

The averaged ablation rate per pulse is estimated by measuring the depth of the laser ablation crater accumulated over 960 pulses, using scanning electron microscopy.

3.2. Experimental results and discussion

Results of the measured expansion velocity of the laser-ablated plume, transmissivity of the laser-ablated plume, the percentage of laser energy scattered from the plume, and the ablation rate per pulse are shown in Figs. 3–5, respectively. According to these results, the laser fluence range used in the experiment can be divided into three regions: the low fluence region with laser fluences between 2.5 J cm^{-2} and 5.2 J cm^{-2}, the medium fluence region with laser fluences between 5.2 J cm^{-2} and 9.0 J cm^{-2}, and the high fluence region with laser fluences higher than 9.0 J cm^{-2}.

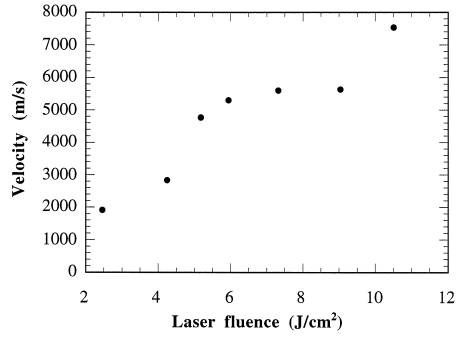

Fig. 3. Velocity of the plume front.

Fig. 3 shows variations of the plume velocity with the laser fluence. These are averaged velocity values within the laser pulse width. The experiment showed that the velocity of the plume front decayed slightly ($\sim 10\%$) within the laser pulse width. The time-averaged velocity increases with the laser fluence increase, from ~ 2000 m s^{-1} at the lowest fluence to ~ 8000 m s^{-1} at the highest fluence. However, the increase of velocity is not monotonous; the velocity is almost a constant in the medium fluence region. The velocity of the plume is determined by the pressure and the temperature at the target surface. The constant velocity in the medium fluence region indicates that the surface temperature is not affected by the increase of the laser fluence in the medium fluence region. Such a constant surface temperature can be explained as a result of explosive evaporation. As discussed earlier, the maximum surface temperature during explosive phase transformation is about $0.9T_c$, the spinodal temperature. Once the laser fluence is high enough to raise the surface temperature to the spinode, further increase of the laser fluence would not raise the surface temperature. On the other hand, in the low fluence region, the velocity increases over 50%. Therefore, the surface temperature increases with the laser fluence increase; heterogeneous vaporization occurs at the surface. At the

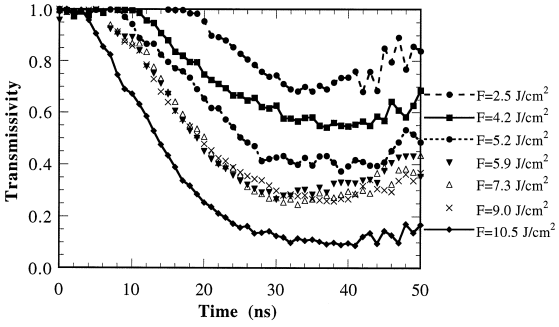

Fig. 4. Transient transmissivity of the laser beam through the laser-ablated plume.

highest laser fluence, the velocity of the plume is higher than that of the middle region. This could be due to a higher absorption rate of the laser energy by the plume, as shown in the transmission measurement (Fig. 4). Absorption of laser energy by the plume further raises the temperature of the plume and increases the plume velocity.

Fig. 4 shows transient transmissivity of the plume at the excimer laser wavelength. The transmissivity remains at '1' for the first several nanoseconds, which is the time duration before evaporation occurs. Transmissivity starts to decrease at an earlier time at higher laser fluences since evaporation occurs earlier at higher fluences. Transmission of the laser beam decreases with the increase of the laser fluence; however, it does not change with the laser fluence in the medium fluence region, i.e., extinction of the laser beam in the plume does not vary with the laser intensity in the medium fluence region. Extinction of the laser beam is determined by the cross-section of the energized atoms, which in turn is determined by the temperature of the plume. As discussed earlier, temperatures of the evaporant in the medium fluence range are all about $0.9T_c$, thus, transmission of the plume stays at a constant value. At the highest laser fluence, transmissivity decreases from that of the middle fluence range, indicating the increase of absorption of laser light by the plume.

Fig. 5 shows the percentage of laser energy scattered from the plume. The size of the scattering center in the plume was measured to be about 120 nm by Xu and Song [12], therefore, scattering is mainly due to large size liquid droplets. Fig. 5 shows that there is almost no scattering (less than 0.5%, the measurement resolution) in the low laser fluence region. Therefore, there is almost no large size liquid droplets in the plume. When the laser fluence is higher than 5.2 J cm^{-2}, the percentage of laser energy scattered by the plume is about 4 to 6%, indicating the existence of liquid droplets in the plume. When explosive phase change occurs, the entire surface layer with a temperature near $0.9T_c$ is evaporated from the target. The high recoil pressure caused by explosive vaporization flushes out liquid from the molten pool. The evaporant during explosive evaporation is thus a mixture of atomic vapor and liquid droplets. Therefore, the result of the scattering measurement provides a direct indication of the transition from heterogeneous evaporation to explosive phase transformation at the laser fluence around 5.2 J cm^{-2}.

Fig. 5 also shows the averaged ablation rate per laser pulse. A substantial increase of the ablation rate occurs at the laser fluence of 5.2 J cm^{-2}; the ablation rate per pulse jumps from about 20 nm at 4.2 J cm^{-2} to about 63 nm at 5.2 J cm^{-2}. This can be viewed as another evidence of the transition from heterogeneous evaporation to explosive evaporation at the laser fluence of 5.2 J cm^{-2}, since the ablation rate increases during explosive evaporation due to ejection of liquid (droplets). Fig. 5 also shows that, when the laser fluence is higher than 5.2 J cm^{-2}, the ablation rate increases slightly with the laser fluence. One reason for this is the increase of melt depth with the laser fluence, therefore, more liquid is expelled from the molten pool during explosive evaporation. Also, as shown in Fig. 2, anomalies of physical properties occur at temperatures higher than $0.8T_c$,

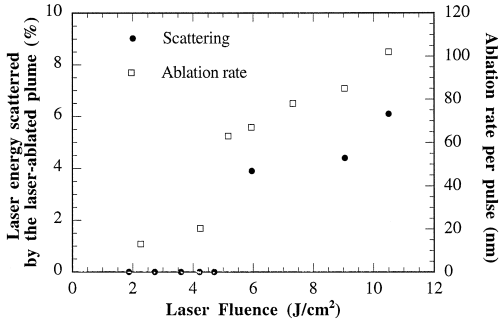

Fig. 5. Percentage of laser energy scattered from the laser-ablated plume and the ablation rate per laser pulse.

the liquid metal becomes less conductive, behaving more like a dielectric material. Therefore, laser radiation could penetrate deeper into the material, extending the optical absorption depth. This effect could further increase the melt depth at higher laser fluences.

4. Conclusions

Mechanisms of PLA at different laser fluence regions were examined experimentally. Time-resolved measurements were performed to determine the velocity of the laser-induced plume, transmission and scattering of the laser beam from the plume and the ablation rate per pulse, at the laser fluences between 2.5 J cm^{-2} and 10.5 J cm^{-2}. The experimental results showed that, when the laser fluence was between 5.2 J cm^{-2} and 9.0 J cm^{-2}, transmissivity of the laser beam in the laser-ablated plume and its expansion velocity changed little. Further, there were drastic variations of the ablation depth and scattering of laser light when the laser fluence was varied across 5.2 J cm^{-2}. All the experimental results consistently showed laser ablation was due to heterogeneous evaporation when the laser fluence was below 5.2 J cm^{-2}, and explosive phase change dominated the evaporation process when the laser fluence was higher than the 5.2 J cm^{-2} threshold value.

Acknowledgements

Support by the National Science Foundation under grant number CTS-9624890 is gratefully acknowledged.

References

[1] F.P. Gagliano, U.C. Paek, Appl. Opt. 13 (1974) 274.
[2] A. Miotello, R. Kelly, Appl. Phys. Lett. 67 (1995) 3535.
[3] R. Kelly, A. Miotello, Appl. Surf. Sci. 96–98 (1996) 205.
[4] M.M. Martynyuk, Russ. J. Phys. Chem. 57 (1983) 494.
[5] W. Fucke, U. Seydel, High Temp. High Press. 12 (1980) 419.
[6] M.M. Martynyuk, Fiz. Gorenniya i Vzryva 13 (1977) 213.
[7] C. Domb, The Critical Point, Taylor and Francis, 1996.
[8] M.M. Martynyuk, Sov. Phys. Tech. Phys. 19 (1974) 793.
[9] M.M. Martynyuk, Russ. J. Phys. Chem. 49 (1975) 1545.
[10] V.A. Bantanov, F.V. Bunkin, A.M. Prokhorov, V.B. Fedorov, Sov. Phys. JETP 36 (1973) 311.
[11] V.P. Skripov, Metastable Liquids, Wiley, New York, 1974.
[12] X. Xu, K.H. Song, J. Heat Transfer 119 (1997) 502.
[13] K.H. Song, X. Xu, Appl. Phys. A 65 (1997) 477.